Accident Analysis and Prevention 113 (2018) 303–316

Contents lists available at ScienceDirect

Accident Analysis and Prevention

journal homepage: www.elsevier.com/locate/aap

Developing a safety heatmap of uncontrolled intersections using both conflict probability and severity

Yingying Ma[a], Xiaoran Qin[a,*], Offer Grembek[b], Zhiwei Chen[a]

[a] South China University of Technology, Department of Transportation Engineering, Guangzhou, Guangdong, 510640, PR China
[b] University of California, Berkeley, Safe Transportation Research and Education Center, Berkeley, CA 94720, United States

ARTICLE INFO

Keywords:
Safety assessment
Uncontrolled intersection
Conflict probability
Conflict severity
Cluster analysis

ABSTRACT

This paper presents a method to assess the safety of uncontrolled intersections considering two major properties of traffic conflicts—conflict probability and severity. This method assesses both the safety level of the entire intersection in addition to the distribution of safety within it. Intersections are modeled by a two-dimensional Cartesian coordinate system and the internal space of intersections is divided into cells. First, the vehicle movement characteristics of an uncontrolled intersection are modeled. Second, the conflict probability of each cell within the intersection is estimated considering the approaching probability and lateral migration probability of vehicles. The quantification of conflict severity is based on kinetic energy loss of potential crashes. Cluster analysis is used to combine conflict probability and severity to model the safety assessment of each cell. Third, the application of the method is discussed, and an overall safety index of intersections is proposed which considers weighted safety level and relative value of areas of different safety levels. Finally, a case study, which includes three different designs, is presented along with safety heatmaps to demonstrate the results. The results not only demonstrate the validity of the model, but also indicate that the proposed method can be applied to: i) safety evaluation of build-up intersections; ii) dangerous position management within an intersection; iii) safety assessment of designed intersections, and iv) safety level comparison among different intersections or various designs for a single intersection. Using this method, engineers and planners can better evaluate and improve the safety of existing or future uncontrolled intersections.

1. Introduction

Intersections are bottlenecks of urban roads and junctions of pedestrian, bicycle and vehicle flows, apart from being nodes where road users change their directions, and traffic conflicts and accidents are concentrated. Statistics reveal that from 2013 to 2015, head-on collisions, broadside collisions and vehicle-pedestrian collisions that occurred primarily at intersections accounted for 47.1% of 9859 traffic accidents in San Francisco (SafeTREC, 2016), while 50% of vehicle crashes in Vitoria, Australia took place at intersections (Cornelissen et al., 2013). The safety problem of intersections has always been of great public concern, and is therefore an extremely important issue in the domain of traffic conflict analysis and safety assessment.

The uncontrolled intersection is common in rural areas of China. There is neither signal control nor stop sign at this kind of intersection to control and manage the traffic flow. Therefore, during the design stage the intersection can be regarded as an uncontrolled intersection. When crossing vehicles arrive at the intersection, the driver can continue through the intersection without any control measures. However, drivers should not only focus on driving through the intersection, but must also pay more attention to the surrounding environment to determine whether they can proceed without any conflicts with other vehicles, pedestrians or bicyclists. This requires increased attention and discretion of drivers compared with those crossing controlled intersections. Unfortunately, this requirement is not always fulfilled due to personal or environmental factors, and therefore conflicts and collisions are more likely to occur at uncontrolled intersections.

Previous research on uncontrolled intersections safety problems analyzed various aspects of driver behavior, including gap acceptance and traffic conflict analysis based on conflict points. When addressing traffic safety problems at uncontrolled intersection based on gap acceptance, video data should be collected and analyzed. Previous studies analyzed the behavior of drivers facing available gaps, how they determined whether it was acceptable or not, and their critical gap out of safety concern. Based on these outcomes, Nagalla et al., 2017 applied support vector machines, decision tree and random forests to predict

* Corresponding author at: South China University of Technology, Department of Transportation Engineering, 381 Wushan Road, Jiaotong Building, Guangzhou, Guangdong 510640, PR China.
E-mail address: xqinad@connect.ust.hk (X. Qin).

https://doi.org/10.1016/j.aap.2018.01.038
Received 25 August 2017; Received in revised form 7 December 2017; Accepted 29 January 2018

the gap acceptance behavior of drivers at uncontrolled intersection, and to evaluate the accuracy of different methods. Maurya et al., 2016 determined the influence of waiting time, occupancy and speed on gap acceptance. Additionally, Kaysi and Abbany, 2007 investigated aggressive driver behavior at uncontrolled intersections, and described the aggressive phenomenon of minor street drivers with high risk. Sayed et al. (1994) built a model to study traffic conflicts in critical situations, and described the behavior of drivers with conventional gap acceptance. Other researches used conflict theory to measure the safety level and conditions at uncontrolled intersections. There are several ways to describe conflict. First, researchers used points to represent the conflict location—for example, conflict point, merging point and separation point (Ceder and Eldar, 2002). This simplified the problem, but was too abstract to accurately express actual crashes. Later, safety surrogate indices were proposed, such as delay and deceleration, which were unable directly reflect the safety problem. Subsequently, two important indices based on field observation were introduced—TTC and PET. These two indices are respectively suitable for measuring rear-end conflicts and angle conflicts and are widely used to address safety problems (Machiani and Abbas, 2016).

Safety assessment, which incorporates direct assessment approaches based on traffic accident statistics, and indirect assessment based on traffic conflict analysis, was introduced in England in 1987. Direct assessment approaches refer to the regression modeling approach, grey evaluation approach and experience modeling approach, which produce results by analyzing data such as accident numbers and accident rates. The generalized linear regression modeling (GLM) approach is now quite common in crash prediction modeling and is used to relate crashes to traffic volume and geometric factors (Lorion and Persaud, 2015). The regression modeling approach conducts a statistical test on variables including traffic volume, delay and conflict categories and achieves results through analysis and prediction (Ma et al., 2010). Some scholars use the binary probit model to measure the risk of hotspots based on the data of crashes per year per kilometer (Ferreira and Couto, 2015). The grey evaluation approach assesses the degree of safety of intersections with gray clustering analysis, using indicators such as Traffic Conflict and Mixed Passenger Car Units (TC/MPCU) as evaluation factors (Niu, 2005; He et al., 2010). Experience modeling approaches are based on large quantities of data. Although indicators of the above methods are direct, their drawbacks are also conspicuous, not only because of their limited assessment results, but also due to their high demand for statistics, long assessment periods and low efficiency.

Indirect assessment approaches based on traffic conflict analysis can be divided into four types based on: statistical data of traffic conflict, hybrid fuzzy clustering, system analysis, and traffic simulation, respectively. Traffic conflict technique is a non-accident based approach widely applied in traffic safety analysis throughout the world. In 1968, traffic conflict was introduced at General Motor and used as a safety assessment approach (Allen et al., 1978). In addition, validity (Minderhoud and Bovy, 2001), estimation methods (Brown et al., 1986; Zhang et al., 2015) and applications (Brown et al., 1986) of traffic conflict technique are also studied. Safety assessment based on statistical data of traffic conflict generally makes evaluations using characteristics of conflict points and conflict probability (Zhang et al., 2015; Wang and Huang, 2014; Lu et al., 2008). Safety assessment approaches based on hybrid fuzzy clustering include two branches, which use fuzzy C-means clustering algorithm (Cheng, 2004) and classical membership (Zhou et al., 2008), respectively. Similarly, safety assessment based on system analysis can also be divided into two branches. Analytic hierarchy process (AHP) (Qu, 2011) and principal component analysis (Zhang, 2012) are used respectively to assess traffic safety comprehensively. Safety assessment based on traffic simulation uses microscopic traffic simulation to obtain traffic conflict data (Sun and Zhao, 2011; Zhou and Huang, 2013).

Studies on safety assessment of uncontrolled intersections are prolific, but several problems have yet to be solved. First, previous studies simplified the vehicle as a particle and the vehicle trajectory as a line, neglecting the actual size of the vehicle, which is inconsistent with real-world circumstances. Second, in most studies the entire intersection is assessed as a whole, based on historical crashes, while details about the intersection, such as traffic conflict, safety degree and the impact of unreasonable design on accidents, are completely omitted, weakening its potential role in intersection design. However, traffic accidents are not a complete indicator of safety of intersections—crash risk is another significant indicator. Therefore, conflict probability and severity should be integrated to ameliorate the safety assessment of intersections. More importantly, the assessment studies or methods mentioned above largely rely on conflict field data or historical accident data. It is obvious that when the design scheme of an intersection needs to be assessed, such studies may not be effective. However, it is significant in conducting safety assessments on intersection schemes before they are put into service—for example, identifying dangerous locations and avoiding design problems in advance. The major goal of this paper is to determine how to assess an intersection in a visual way closer to reality, particularly one that can be applied to an intersection design scheme without any operation field data. The findings in this paper can provide reference and support for road planning and design.

This paper presents a safety assessment approach of uncontrolled intersections considering conflict probability and severity. Previous works generally conducted research from a single aspect. However, conflict probability and severity both affect a crash. Conflict probability shows how likely a crash is to happen at a certain position within the intersection, while conflict severity reflects the type of crash it may be and how serious the crash is. Intersections are divided into cells to detail the safety information of the intersections. The safety level of each specific cell within the internal space of an intersection can be calculated and shown in a visualization picture. To evaluate the safety level of the entire intersection, an overall safety assessment method for intersections is presented, which could be used for comparing safety situations of multiple intersections or alternatives for a single intersection.

2. Modeling movement characteristics of vehicles at uncontrolled intersections

The running characteristics of vehicles at uncontrolled intersections determine the distribution of traffic conflicts, and have a crucial impact on the safety level of intersections. Therefore, the analysis and modeling of vehicle movement characteristics are the foundation work of safety assessment.

2.1. Assumptions

This paper takes a four-leg intersection as an example, but the methodology can also be applied to intersections with various geometric shape and lane width. The basic assumptions are as follows:

i) Only automobile (cars only, buses and trucks are excluded) are taken into consideration, the impacts of pedestrian and non-motor vehicle are excluded.
ii) Vehicles stay in one lane and do not change lanes when they pass through intersections.
iii) Width of lanes at each approach and exit are the same.
iv) Only conflicts in the internal space of the intersection are considered, merging and diverging conflicts at approaches and exits of the intersection are excluded.

2.2. Modeling intersection and vehicle trajectories

The modeling process includes building a two-dimensional Cartesian coordinate system: the center of the intersection is defined as the coordinate origin, the center line of the west-to-east road as the x-

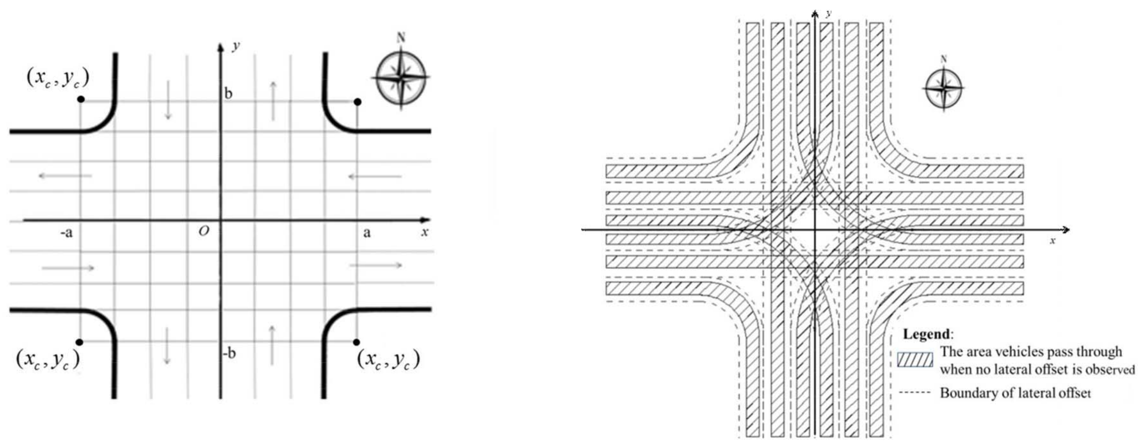

(a) Coordinate system of intersection and grid processing **(b) Vehicle trajectories, conflict areas sketch**

Fig. 1. Modeling uncontrolled intersections and vehicle trajectories.

axis, and that of the south-to-north road as the y-axis. Assuming that the length of intersection is $2a$, and the width is $2b$, the length and width are equally divided into n parts separately: $-a = x_0 < \ldots < x_n = a$, $-b = y_0 < \ldots < y_n = b$, so that the entire intersection is divided into N cells (Fig1(a)), where $N = n^2$. As the number of cells$N \to \infty$, the area of each cell $s \to 0Cell(ij)$ denotes the *ith* from west and *jth* from south cell (abbreviated to *ij* in equations below). Let (x_{ij}, y_{ij}) represents the coordinate of $Cell(ij)$, which is the centroid of $Cell(ij)$, and equals to $(x_i - \frac{a}{n}, y_j - \frac{b}{n})$ while $i, j = 1, 2, \ldots, n$. According to the design of the intersection diversion route (Wang, 2013), the trajectories of the straight forward moving vehicles are generally within the range between the links of the approach and exit lane line, while turning vehicles move in the curved diversion route which is at least the same width as the lane (Hu, 2009). Taking the width of vehicles into consideration, the vehicle trajectories of each approach and conflict areas are drawn on the simplified intersection plan (Fig. 1(b)). The description of the trajectory can be applied not only to intersections with the same lane width of approach and exit, but also to those of different lane widths; the parameters' value of trajectory functions is the primary difference.

Consider two situations—one is a simple case, the lane number of the corresponding approach and exit are the same, and the trajectory can be described by the following method:

Counted from the coordinate axis, if there are straight forward vehicles running on the kth lane (including the straight forward lanes as well as straight-turning lanes), the straight forward trajectory scope from the north approach is shown as Eq. (1), (where Adenotes the width of median separator). For the east approach, replace x by y, while the scope of south and west approach are multiplied by -1 on both sides.

$$\Phi_x = \{x\colon \frac{A}{2} + k*D \le x \le \frac{A}{2} + (k-1)*D\} \tag{1}$$

Commonly in China, to reduce the conflict in space, the right-turn lane (or mixed lane allowing right turning vehicles) is located on the right hand side of the approach, and for this example suppose that the right-turning vehicles run along the designed turning radius on its direction. The left-turn lane is located on the left hand side. The turning trajectory range of each approach is shown as Eq. (2).

$$(x - x_c)^2 + (y - y_c)^2 = R^2,\ \ R \in \left[R_d - \frac{D}{2}, R_d + \frac{D}{2}\right] \tag{2}$$

where $R$is the radius range, while R_d is the design radius of left or right turn trajectories; and D is the width of lane; x_c, y_c are the abscissa and ordinate of arc trajectory center, which can be regarded as the center of design turning radius. For example, the turning (kth lane) trajectory center of east approach is $\left(R_d - \frac{(2k-1)D}{2}, -R_d + \frac{(2k-1)D}{2}\right)$, and center of other approaches should be multiplied by -1 according to the quadrant.

In the other situation, the lane number does not match, which implies that the vehicles run along the same direction and may leave the intersection in different exit lanes. However, the main logic is consistent with the previous situation—two or more trajectories in the same direction can also be expressed as functions. The application is shown as Section 5 Verification.

2.3. Modeling vehicle lateral migration

The lateral migration occurs frequently when vehicles are moving in a lane, and is caused by driver operating behavior. According to data collection and statistics, it is proposed that the offset (distance between center line of vehicle and lane) of vehicles on a curve in the road generally follows the normal distribution (Lin et al., 2011), and later, it is shown that this finding can also be applied to straight forward moving vehicles (Wang et al., 2016). The same conclusions are reached using driving characteristics analysis (Lin, 2010). According to the findings from previous literature mentioned above (Lin et al., 2011), the probability decreases with the rise of the lateral offset; the probability density function of lateral offset follows the normal distribution.

There are three potential cases when vehicles are moving in a single lane (Fig. 1a). Case 1 represents the condition that the center line of vehicle and lane coincide with each other; Case 2 is the condition in which the vehicle's left edge coincides with the left boundary of the lane; while Case 3 represents the coincidence of right edge of the vehicle and right boundary of the lane. Therefore, the lane is divided into three zones as shown in Fig. 2. Regardless of which direction the vehicle migrates, it occupies part of the lane (Z_2 area) at all times. However, whether areas Z_1 and Z_3 on both sides are occupied depends on the lateral offset, and its probability can be determined by integration of density function.

The lateral migration behavior of turning vehicles is similar to straight forward moving vehicles (Fig. 2b). In particular, the centerline in the design of a turning route is regarded as the location with little offset. The reference lines of both sides are the tangents of the vehicle edge, and are compared with the tangent of turning diversion route during the analysis of lateral offset.

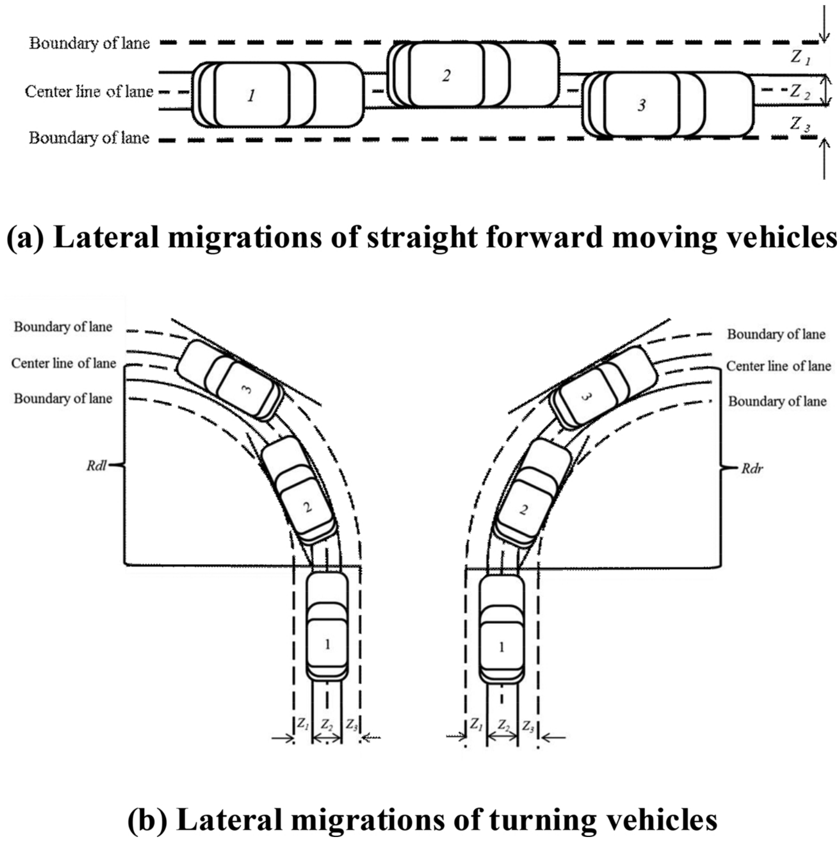

Fig. 2. Lateral migrations illustration of vehicles moving in lanes.

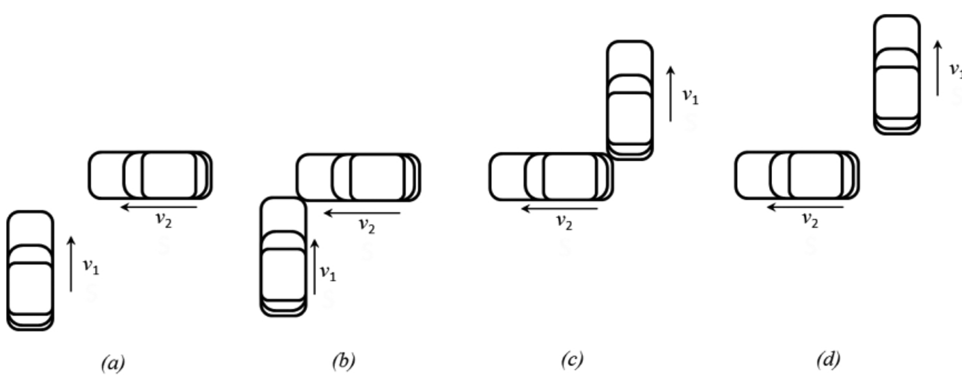

Fig. 3. Conflict process illustration of two vehicles.

3. Methodology

3.1. Data collection and preparation

There are four categories of data utilized for this paper: geometry information of intersections, velocity of vehicles at intersections, traffic volume of each approach, and vehicle-related parameters.

3.2. Conflict probability prediction

Conflict is generally defined as a situation in which two or more road users will collide if neither of them makes an evasive maneuver. The definition used in this paper is more strict—a conflict occurs when two or more vehicles arrive at the same cell the same time. The concepts can be defined as follows: P_R is the approaching probability which is related to the arrival rate, and represents the probability that the vehicle passes the trajectory section to which some cell belongs. P_D is the lateral migration probability, and represents the probability that the vehicle migrates to some cell at one trajectory section. Therefore, the probability of a vehicle appearing at $Cell(ij)(P_{A_{ij}})$ can be expressed as the product of approaching probability and lateral migration probability for the same cell.

$$P_{A_{ij}} = P_{R_{ij}} \times P_{D_{ij}} \tag{3}$$

3.2.1. Approaching probability

Previous research indicates that the Poisson distribution can properly fit vehicle arrival (Hu, 2009). It can also be applied to express the approaching probability of $Cell(ij)$ during the observation period t. (Eq. 4)

$$P_{R_{ij}} = 1 - P(X = 0) = 1 - e^{-\lambda_k t} \tag{4}$$

where $\lambda_k pcu/h$) is the arrival rate of vehicles on trajectory k, and t(s) is the observation period. From condition (b) to (c) shown in Fig. 3, the running time of vehicle 1 is $t_1 = \frac{L+B}{v_1}$, while that of vehicle 2 is $t_2 = \frac{L+B}{v_2}$. Therefore, the observation period should be the minimum time interval during which two vehicles do not experience a conflict. (Eq. 5)

$$t = \min\left(\frac{L+B}{v_1}, \frac{L+B}{v_2}\right) \tag{5}$$

where v_1 and $v_2$are the vehicle velocities that may conflict

The approaching probability of $Cell(ij)$ during the observation period is obtained by substituting Eq. (5) into Eq. (4).

$$P_{R_{ij}} = 1 - e^{-\lambda_k \min\left(\frac{L+B}{v_1}, \frac{L+B}{v_2}\right)} \tag{6}$$

3.2.2. Lateral migration probability

The derivation equation of lateral migration probability $P_{D_{ij}}$ is obtained on the basis of the probability density function and interval segmentation.

$$P_{D_{ij}} = \begin{cases} \int_{l_1}^{u_1} \frac{1}{\sqrt{2\pi}\sigma} e^{-\frac{(x-\mu)^2}{2\sigma^2}} dx, & Cell(ij) \in Z_1 \\ 1, \ Cell(ij) \in Z_2 \\ \int_{l_2}^{u_2} \frac{1}{\sqrt{2\pi}\sigma} e^{-\frac{(x-\mu)^2}{2\sigma^2}} dx, & Cell(ij) \in Z_3 \end{cases} \tag{7}$$

where $u_i$and $l_i (i = 1, 2$ and $l_i < u_i)$are the bounds of integration which represent the lateral offset.

Since lateral migration probability refers to the probability that a certain cell in the lane is occupied by vehicles, the bounds should be the range of lateral offset when the cell is occupied. Suppose there is a four-leg uncontrolled intersection with three lanes at each approach, one straight forward lane, one left-turning lane and right-turning lane. Take the east approach as an example to solve the integration bounds. Assume that $Cell(ij)$ is the cell within the trajectory scope in the east straight forward lane (2nd lane). The straight forward lanes and turning lanes of other approaches are similar:

If $Cell(ij)$falls in Z_2, which means $y_{ij} \in \left[2D - B + \frac{A}{2}, D + B + \frac{A}{2}\right]$, then $P_{D_{ij}} = 1$;

If $Cell(ij)$is in Z_1, which means $y_{ij} \in \left(D + B + \frac{A}{2}, 2D + \frac{A}{2}\right]$, then:

When a vehicle migrates to the location so that its right (or left) edge coincides with left (or right) edge of a cell, the vehicle occupies that cell at the first time. This corresponds to the lower bound of integration (Eq. (8)).

$$l_1 = y_{ij} - y_0 = y_{ij} - \frac{3D + B + A}{2} \tag{8}$$

As the vehicle moves toward the right (or left), and when the right (or left) edge of the vehicle coincides with the right (or left) lane line, the cell is still occupied. This corresponds to the upper bound (Eq. (9)).

$$u_1 = y_m - y_0 = \frac{D - B}{2} \tag{9}$$

The lateral migration probability of cells in Z_1 is obtained (Eq. (10)) by substituting Eq. (8) and Eq. (9) into Eq. (7).

$$P_{D_{ij}} = \int_{y_{ij} - \frac{3D+B+A}{2}}^{\frac{D-B}{2}} \frac{1}{\sqrt{2\pi}\sigma} e^{-\frac{(y-\mu)^2}{2\sigma^2}} dy \tag{10}$$

Similarly, if $Cell(ij)$ falls into Z_3, meaning $y_{ij} \in \left[D + \frac{A}{2}, 2D - B + \frac{A}{2}\right)$, then

$$P_{D_{ij}} = \int_{y_{ij} - \frac{3D-B+A}{2}}^{\frac{D-B}{2}} \frac{1}{\sqrt{2\pi}\sigma} e^{-\frac{(y-\mu)^2}{2\sigma^2}} dy \tag{11}$$

According to the analytical method shown above, the straight lane lateral migration probabilities of the four approaches are shown as Eq. (12).

$$P_{D_{ij}} = \begin{cases} \int_{y - \frac{3D+B+A}{2}}^{\frac{D-B}{2}} \frac{1}{\sqrt{2\pi}\sigma} e^{-\frac{(y-\mu)^2}{2\sigma^2}} dy, \ y \in \left(D + B + \frac{A}{2}, 2D + \frac{A}{2}\right] \\ 1, \quad y \in \left[2D - B + \frac{A}{2}, D + B + \frac{A}{2}\right] \\ \int_{y - \frac{3D-B+A}{2}}^{\frac{D-B}{2}} \frac{1}{\sqrt{2\pi}\sigma} e^{-\frac{(y-\mu)^2}{2\sigma^2}} dy, \ y \in \left[D + \frac{A}{2}, 2D - B + \frac{A}{2}\right) \end{cases} \tag{12}$$

where the value of y: east approach $y = y_{ij}$, west approach$y = -y_{ij}$, north approach$y = -x_{ij}$, south approach $y = x_{ij}$.

The turning lateral migration probabilities are shown as Eq. (13).

$$P_{D_{ij}} = \begin{cases} \int_{R_w - \frac{B}{2} - R_{dw}}^{\frac{D-B}{2}} \frac{1}{\sqrt{2\pi}\sigma} e^{-\frac{(R_w-\mu)^2}{2\sigma^2}} dR_w, \ R_w \in \left(R_{dw} + B - \frac{D}{2}, R_{dw} + \frac{D}{2}\right] \\ 1, \quad R_w \in \left[R_{dw} - B + \frac{D}{2}, R_{dw} + B - \frac{D}{2}\right] \\ \int_{\left|R_w + \frac{B}{2} - R_{dw}\right|}^{\frac{D-B}{2}} \frac{1}{\sqrt{2\pi}\sigma} e^{-\frac{(R_w-\mu)^2}{2\sigma^2}} dR_w, \ R_w \in \left[R_{dw} - \frac{D}{2}, R_{dw} - B + \frac{D}{2}\right) \end{cases} \tag{13}$$

Where w denotes l or r. When w denotes l, the value ofR_{dl} is: east approach$R_{dl} = |(x_m - x_n)^2 + (y_m - y_0)^2|^{1/2}$, west approach$R_{dl} = |(x_m - x_0)^2 + (y_m - y_n)^2|^{1/2}$, north approach $R_{dl} =|(x_m - x_n)^2 + (y_m - y_n)^2|^{1/2}$, south approach $R_{dl} = |(x_m - x_n)^2 + (y_m - y_0)^2|^{1/2}$. When w denotes r, the value ofR_{dr}: east approach $R_{dr} = |(x_m - x_n)^2 + (y_m - y_n)^2|^{1/2}$, west approach $R_{dr} = |(x_m - x_0)^2 + (y_m - y_0)^2|^{1/2}$, north approach $R_{dr} =|(x_m - x_0)^2 + (y_m - y_n)^2|^{1/2}$, south approach $R_{dr} =|(x_m - x_n)^2 + (y_m - y_0)^2|^{1/2}$

3.2.3. Conflict probability

As the trajectories diagram shows, there are up to three trajectories across the same cell, designated as $k = a, b, c$. Ignoring the infinitesimal of higher order, the final conflict probability is defined as Eq. (14).

$$P_{C_{ij}} = P_{A_{ij}}^a \times P_{A_{ij}}^b + P_{A_{ij}}^b \times P_{A_{ij}}^c + P_{A_{ij}}^a \times P_{A_{ij}}^c \tag{14}$$

where $P_{A_{ij}}^k$ is the probability of a vehicle on trajectory k appears at $Cell(ij)$ (Eq. (3)).

3.3. Conflict severity assessment

Previous research provided several quantitative methods for traffic conflict severity. Quantitative severity value was estimated based on: time to collision and non-complete braking time (Lu et al., 2012), velocity and time to conflict (Laureshyn et al., 2010), and crash occurrence probability as well as expected severity demonstrated by kinetic energy (Alhajyaseen, 2015). According to previous studies, the energy loss of a potential crash is a feasible way to demonstrate the severity of conflict. Given the worst case scenario, the assumptions are as follows:

i) The weight of vehicles is almost the same.
ii) Before a crash, vehicles fail to adopt braking measures and maintain constant velocity.
iii) During a crash, the resultant internal force of the system is much larger than the external force.

There are at least two trajectories for each conflict point, and the velocity vector can easily be obtained in terms of the conflict trajectories. Decomposing the velocity of the crash vehicles to x and y-axes, combined with the theory of momentum conservation, the kinetic energy loss model is established. Kinetic energy loss per unit mass of each cell at the intersection can be obtained using Eq. (16).

$$\Omega = \frac{\Delta E}{\overline{m}} = \frac{1}{4}(v_1^2 + v_2^2) - \frac{1}{2} v_1 v_2 \cos(\theta_1 - \theta_2) \tag{16}$$

where Ω denotes the conflict severity, $\overline{m}$ is the average mass of crash vehicles, v_1 and v_2 are the velocities of each vehicle prior to the crash, while θ_1, θ_2 are the separate angles of vehicle velocity which are measured counterclockwise from the positive x-axis.

Table 1
Definition and representation of main parameters.

Data Categories	Main Content	Symbol	Collection Method
Geometry information of Intersections	Width of lanes	D	Data of field measurement
	Width of median separators	A	
	Radius of curbs	R_0	
	Design radius of left-turn vehicles	R_{dl}	
	Design radius of right-turn vehicles	R_{dr}	
Vehicle velocity (left-turn, straight and right-turn)	Velocity of east approach	V_{el}, V_{es}, V_{er}	Investigation velocity or design velocity
	Velocity of west approach	V_{wl}, V_{ws}, V_{wr}	
	Velocity of south approach	V_{sl}, V_{ss}, V_{sr}	
	Velocity of north approach	V_{nl}, V_{ns}, V_{nr}	
Traffic volume (left-turn, straight and right-turn)	Arrival rate of east approach	λ_{el}, λ_{es}, λ_{er}	Design hourly volume or investigated hourly volume
	Arrival rate of west approach	λ_{wl}, λ_{ws}, λ_{wr}	
	Arrival rate of south approach	λ_{sl}, λ_{ss}, λ_{sr}	
	Arrival rate of north approach	λ_{nl}, λ_{ns}, λ_{nr}	
Vehicle related parameters	Length of standard vehicles	L	Related literature or investigation statistics
	Width of standard vehicles	B	
	Average lateral offset	μ	
	Lateral offset variance	σ	

Table 2
Whitenization value of the two indicators.

Indicators	Whitenization Value			
	λ_1	λ_2	λ_3	λ_4
Conflict probability[a]	0	0.001	0.025	0.036
Conflict severity(J/kg)[b]	0	50	100	150

[a] Obtained from the cumulative frequency curve of TC/MPCU (Pei, 2007).
[b] Obtained from previous research (Zhang et al., 2012).

Four levels of conflict severity are defined based on the statistics of energy loss and crash severity: slight conflict, general conflict, severe conflict, and serious conflict. The severity level of each cell can be determined according to its kinetic energy loss per unit mass (Zhang et al., 2012).

3.4. Integration of conflict probability and severity using cluster method

For the safety assessment, conflict probability and conflict severity are two important indicators, therefore, it is necessary to take both into consideration (Alhajyaseen, 2015). The combination of these two factors could provide decision makers and road design engineers with better support and guidance.

The cluster analysis classifies the object into n categories using the whitenization weight function of different cluster indicators, thus achieving determination of cluster objects. This method can synthesize the impacts of multiple indices and has the advantage of clear algorithm and strong practicality, particularly when there is an explicit basis of whitenization value (Chen and Yin, 2013). In this paper, the cluster analysis method is properly applied to satisfy the demand of a large number of cells that need to be assessed, along with two indicators: conflict probability and severity.

According to previous research, four safety levels are defined by conflict probability (Pei, 2007) and conflict severity (Zhang et al., 2012), respectively. Therefore, four safety levels are used in this paper: level I denotes safe, level II denotes marginally safe, level III denotes dangerous, and level IV denotes seriously danger. The whitenization values are shown in Tables 1 and 2.

Whitenization values are used to solve the corresponding functions (Eq. (17)). (z is the number of indicator, x is independent variable).

$$f_z^1(x)=\begin{cases}1 & (x<\lambda_1)\\ \frac{\lambda_1-x}{\lambda_2-\lambda_1} & (\lambda_1<x<\lambda_2)\\ 0 & (x>\lambda_2)\end{cases}\quad f_z^2(x)=\begin{cases}0 & (x<\lambda_1)\\ \frac{x-\lambda_1}{\lambda_2-\lambda_1} & (\lambda_1<x<\lambda_2)\\ \frac{x-\lambda_2}{\lambda_3-\lambda_2} & (\lambda_2<x<\lambda_3)\\ 0 & (x>\lambda_3)\end{cases}$$
$$f_z^3(x)=\begin{cases}0 & (x<\lambda_2)\\ \frac{x-\lambda_2}{\lambda_3-\lambda_2} & (\lambda_2<x<\lambda_3)\\ \frac{\lambda_4-x}{\lambda_4-\lambda_3} & (\lambda_3<x<\lambda_4)\\ 0 & (x>\lambda_4)\end{cases}\quad f_z^4(x)=\begin{cases}0 & (x<\lambda_3)\\ \frac{x-\lambda_3}{\lambda_4-\lambda_3} & (\lambda_3<x<\lambda_4)\\ 1 & (x>\lambda_4)\end{cases} \tag{17}$$

The cluster weight can be obtained from experts who are experienced in the field of traffic conflict. The cluster coefficient of each cell is

Table 3
Major performance metrics and usage.

Performance Metrics	Explanation	Usage
Area of each safety level	Total area of cells in each safety level.	Provides detailed information on each safety level within an intersection. The larger the area with lower safety levels, the lower the safety level of the entire intersection. Could be used to compare the effects of alternatives for an intersection.
Relative value of area	Area of each safety level divided by the area of the safest level.	Provides a relative value of each safety level unaffected by the area of an intersection. Could be used to compare intersections or alternatives for one intersection.
Number of conflict zones	Conflict zones can be observed by visualization of cells' safety assessments. Adjacent cells with safety levels of II to IV could be seen as a conflict zone. Drivers may be distracted by numerous conflict zones, resulting in compromised safety.	Provides information on conflict areas, could be used to make comparisons among intersections or alternatives for a single intersection.
Overall safety index	A relative safety index obtained by weighted relative values of areas of each safety level	Provides an overall safety assessment of intersections, could be used in safety comparisons among intersections or alternatives for one intersection, and for conflict hotspot identification.

Table 4
Parameter values of the intersection.

Parameter	D(m)	A(m)	L(m)	B(m)	λ_{nr}(veh/s)	λ_{ns}(veh/s)	λ_{nl}(veh/s)
Value	3	0	4	2	0.2	0.56	0.1
Parameter	R_{wr}(m)	R_{nr}(m)	R_{el} (m)	R_{nl}(m)	λ_{el}(veh/s)	λ_{es}(veh/s)	
Value	3	6	6.5	6.5	0.4	0.2	
Parameter	φ_1	φ_2	φ_3	φ_4	λ_{ws}(veh/s)	λ_{wr}(veh/s)	
Value	1	4	7	10	0.05	0.1	

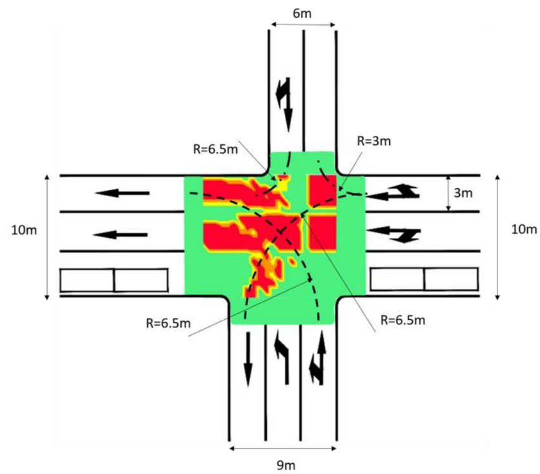

Legend	Color	Safety level	Description	Legend	Color	Safety level	Description
	Green	I	Safe		Orange	III	Dangerous
	Yellow	II	Marginally safe		Red	IV	Seriously dangerous

Fig. 4. Safety heatmaps of Jianshe Road-Beijiaochang Road intersection.

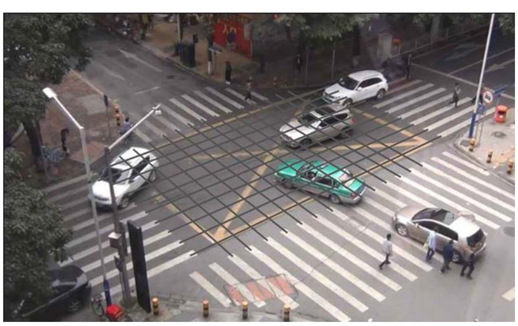

Fig. 5. Video analysis sketch of Jianshe Road-Beijiaochang Road intersection.

shown in Eq. (18).

$$\sigma^k_{Cell(ij)} = \sum_{z=1}^{2} f^k_z(Cell(ij)_z) \times n_z \tag{18}$$

where $\sigma^k_{Cell(ij)}$ denotes the coefficient that $Cell(ij)$ belongs to the kth cluster, $Cell(ij)_z$ is the zth indicator value of $Cell(ij)$, η_z the weight of zth indicator which could be determined by experts' experience, $f^k_z(x)$ the whitenization weight function of x.

The safety level of $Cell(ij)$ is $\sigma^{k^*}_{Cell(ij)} = \max\{\sigma^k_{Cell(ij)}\}$, which means the object $Cell(ij)$ belongs to the k^*th class and the safety level is k

4. Applications

The above analysis focuses on the safety assessment of each cell in the intersection which also provides basic data for intersection safety assessment. Several performance metrics can be extracted to assess the entire intersection based on safety level distribution within intersections.

4.1. Definition of relative value of area

When assessing various intersections, the intersection area and condition of grid process may not be the same. This phenomenon necessitates the conversion of the absolute value to a relative value to make comparisons among intersections possible. Therefore, areas of each safety level category are divided by the area with the safest level S_1, and then relative values are generated which are independent to the area. The symbol ρ_k represents the relative value of area with level k.

$$\rho_k = \frac{S_k}{S_1} = \left(\frac{2a \times 2b}{N} \times n_k\right) \Big/ \left(\frac{2a \times 2b}{N} \times n_1\right) = \frac{n_k}{n_1} \tag{19}$$

where n_k denotes to the number of cells belonging to kth level; $2a$, $2b$ are the length and width of intersection.

4.2. Definition of overall safety index

Cells of different safety levels exert different influence on the overall safety status of the entire intersection. Instead of directly using the areas of cells which belong to a different level, the influence should be embodied by weight. The overall safety assessment model could be built by weighted summation of relative value of areas as shown in Eq. (20).

$$K = \sum_{k=1}^{4} \rho_k \times \varphi_k \tag{20}$$

where K is the overall safety index of the intersection; φ_k is the weight

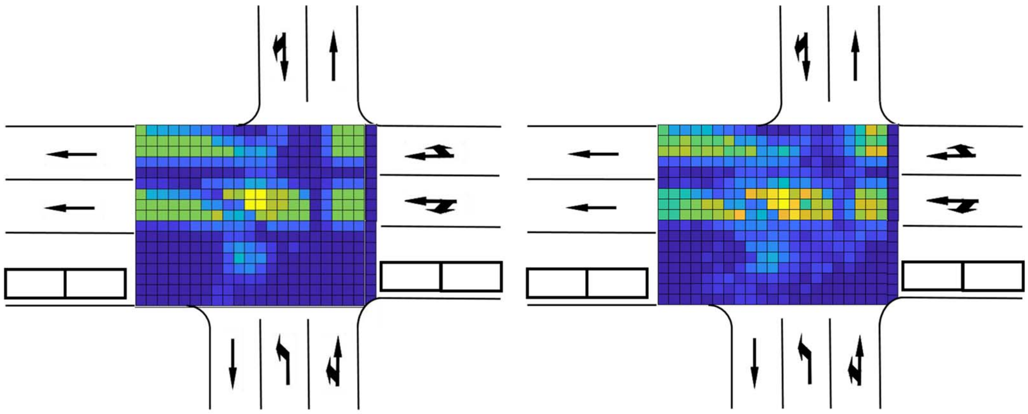

a) The distribution of conflict frequency obtained by the proposed method

b) The distribution of conflict frequency obtained by video conflict observation

Fig. 6. The distribution results of conflict frequency obtained by the two methods.

Table 5
Safety assessment results of the intersection.

Level I	Level II	Level III
Area (m^2) 47.25	Relative area 1	Area (m^2) 6.5

Level IV		Entire intersection		
Area (m^2)	Relative area	Total area(m^2)	Overall index	Number of conflict areas
41.25	0.8730	99	10.8730	4

of kth level, which should be obtained by cost analysis, social investigation and calculation of accident loss. The lower the safety level is, the more loss and influence an accident exerts, and the higher the weight should be. ρ_k is the relative value of an area with level k, which is shown in Eq. (19).

5. Verification

5.1. Background

The traffic flow crossing the uncontrolled intersection, Jianshe Road-Beijiaochang Road intersection in Guangzhou is moderate. The road on the north side is a one-way road with two lanes. One is straight-left lane and the other is straight-right lane. The east-side road is a two-lane road, while the west-side road is a two-way road with three lanes. The west approach has a left-turning lane and a straight-left lane. The geometric and vehicle parameters of the intersection are shown in Tables 3 and 4.

5.2. Result of the proposed method

The safety heatmap is obtained (see Fig. 4) after applying the proposed safety assessment method to this intersection.

According to the analysis of the proposed method, it is obvious that the safety status of this intersection is serious. Dangerous areas occupy over 40% of the total area, and the overall index is up to 10.87, which is normally 2–3 based on the results of other intersection using the proposed method. This demonstrates the high collision risk of this intersection.

5.3. Result of the video conflict detection

After recording 108 min at this intersection during peak hours and analyzing the conflicts in the video, over 300 incidences of conflicts are observed and the frequencies of conflict that occurred on each cell within the intersection are obtained. If possible conflict vehicles appear in the trajectory range of one vehicle, and this vehicle takes avoidance actions because of the conflict vehicles, this can be recorded as a conflict. The possible conflict area includes cells that the trajectory ranges of two conflict vehicles both cover. The video processing method is shown as Fig. 5.

The conflict probability in this paper is the probability that vehicles arrive at the same time in unit observation time. Therefore, to better compare with the video analysis result, the probability should be converted to the frequencies of conflict that occurred on each cell during the 108 min calculated by the proposed method. This can be obtained by the product of conflict probability and the number of unit observation time in 108 min. The conflict frequency comparison processed by MATLAB is shown in Fig. 6. The difference between the two figures is shown in Tables 5 and 6.

After comparing the two conflict frequency distribution maps, it is determined that 32.6% cells in the intersection have the same conflict frequency, when separately calculated by the proposed method and the video conflict detection, while the cells whose frequency difference is less than 4 occupy 76.3%. Therefore, the conflict distribution results obtained by the proposed method and the video conflict detection have great similarity in distribution location and corresponding color. The differences are mainly reflected in two aspects: one is that the actual conflict frequency distribution obtained by video detection is more scattered than that shown in the result of the proposed method. This could be due to violation behaviors such as not driving inside a lane. However, the conflict frequency caused by violation behaviors is

Table 6
The difference between the result of the proposed method and reality.

Difference Value	Number of cell	Ratio in total area
0 (The same)	129	32.6%
< = 2	205	51.8%
< = 3	242	61.1%
< = 4	302	76.3%

Table 7
The constant parameters value in the case study.

Parameter	D(m)	A(m)	L(m)	B(m)	R_{dl}(m)	R_{dr}(m)	η_1
Value	3.5	1	4	2	21.75	11.25	0.6
Parameter	φ_1	φ_2	φ_3	φ_4	μ	σ	η_2
Value	1	4	7	10	0.011	0.572	0.4

relatively low, generally limited to one or two conflicts. The other aspect is that the actual conflict frequency of the same cell is less than the result obtained by the proposed method. This may be a result of the short recording time and limited sample size.

In conclusion, the comparison results above indicate that the conflict distributions obtained by the proposed method and the video detection are similar. The safety status of this intersection is assessed as seriously dangerous. The results demonstrate that the safety assessment method proposed in this paper is feasible and reliable in intersection safety problems. Moreover, using this method can be more convenient than previous methods.

6. Case study

6.1. Background

The uncontrolled intersection in Kunming China, Yanjiang North Road and Xingfu Road, has lower flow in the north-south direction, but greater flow in the west-east direction due to the commercial facilities along Xingfu Road. The safety heatmap is used to analyze the safety conditions of different traffic management measures and to determine the relative optimal scenario that improves the present safety situation of this uncontrolled intersection. The relative parameters are obtained from field measurement and simulation (Table 5).

To visually present the assessment results, this paper assigns four colors: green, yellow, orange and red, to represent safety levels I-IV. The intersection is divided into 1681 square cells, each with a length of 1m. The assessment results were calculated by MATLAB software.

The traffic management measures of uncontrolled intersection include spatial division and traffic parameters control. For grade intersections, the spatial division measure mainly refers to channelization, which has been conducted in this case study. Therefore, only measures of traffic parameter control are taken into consideration. The traffic parameters include vehicle flow and design velocity.

6.2. Flow control

Evacuating and guiding upper reaches can achieve flow control. The flow control can be regarded as the control of arrival rate. The flow volume of each direction is adjusted, while the design velocity is kept as unchanged. Based on the field survey, the present arrival rate and safety improvement scenarios as well as assessment results are shown in Tables 7 and 8, and the safety heatmap is shown in Fig. 7. Scenario 0 is the existing scenario, and the scenario 1–4 reduce the arrival rate of east, west, south and north approach.

According to results above, it is obvious that the relative area of levels III and IV are smaller than the existing scenario, which means traffic flow control is helpful in reducing the area of more dangerous levels. When the flow volume of each direction is decreased proportionately, the direction with larger flow previously is additionally reduced, but the safety improvement effect is improved, for example, scenario 1 and 2. The safety improvement effect along the left-turn trajectory of one approach is significant when the flow of this direction is reduced. Generally speaking, the flow control measure only improves the overall safety index, however it cannot reduce the conflict area number. Comparing the existing scenario and scenario 2, which is the most effective scenario, the overall safety index is only reduced by 3%.

Moreover, to determine how safety condition changes with the flow, the flow of each approach increases from 0 to 3600 pcu/h with a stepsize of 36 (0.01pcu/s), and note how the overall safety index

Table 8
Parameter values and safety assessment results of flow control measures.

Flow control scenario (veh/s)

No.	East approach			West approach			South approach			North approach		
	Left	Straight	Right	Left	Straight	Right	Left	Straight	Right	Left	Straight	Right
0	0.477	0.477	0.477	0.498	0.498	0.498	0.263	0.263	0.263	0.289	0.289	0.289
1	0.217	0.237	0.207	0.498	0.498	0.498	0.263	0.263	0.263	0.289	0.289	0.289
2	0.477	0.477	0.477	0.228	0.249	0.218	0.263	0.263	0.263	0.289	0.289	0.289
3	0.477	0.477	0.477	0.498	0.498	0.498	0.125	0.132	0.110	0.289	0.289	0.289
4	0.477	0.477	0.477	0.498	0.498	0.498	0.263	0.263	0.263	0.139	0.145	0.125

Safety assessment results

Scenario No.		0 (Existing)	Scenario 1	Scenario 2	Scenario 3	Scenario 4
Level I	Area(m^2)	1513	1513	1513	1515	1515
	Relative value	1	1	1	1	1
Level II	Area(m^2)	95	105	108	100	103
	Relative value	0.0628	0.0694	0.0714	0.0660	0.0680
Level III	Area(m^2)	7	8	5	6	7
	Relative value	0.0046	0.0053	0.0033	0.0040	0.0046
Level IV	Area(m^2)	66	55	55	60	56
	Relative value	0.0436	0.0364	0.0364	0.0396	0.0370
Entire intersection	Total area(m^2)	1681	1681	1681	1681	1681
	Overall index	1.7198	1.6781	1.6722	1.6878	1.6739
	Number of conflict areas	8	8	8	8	8

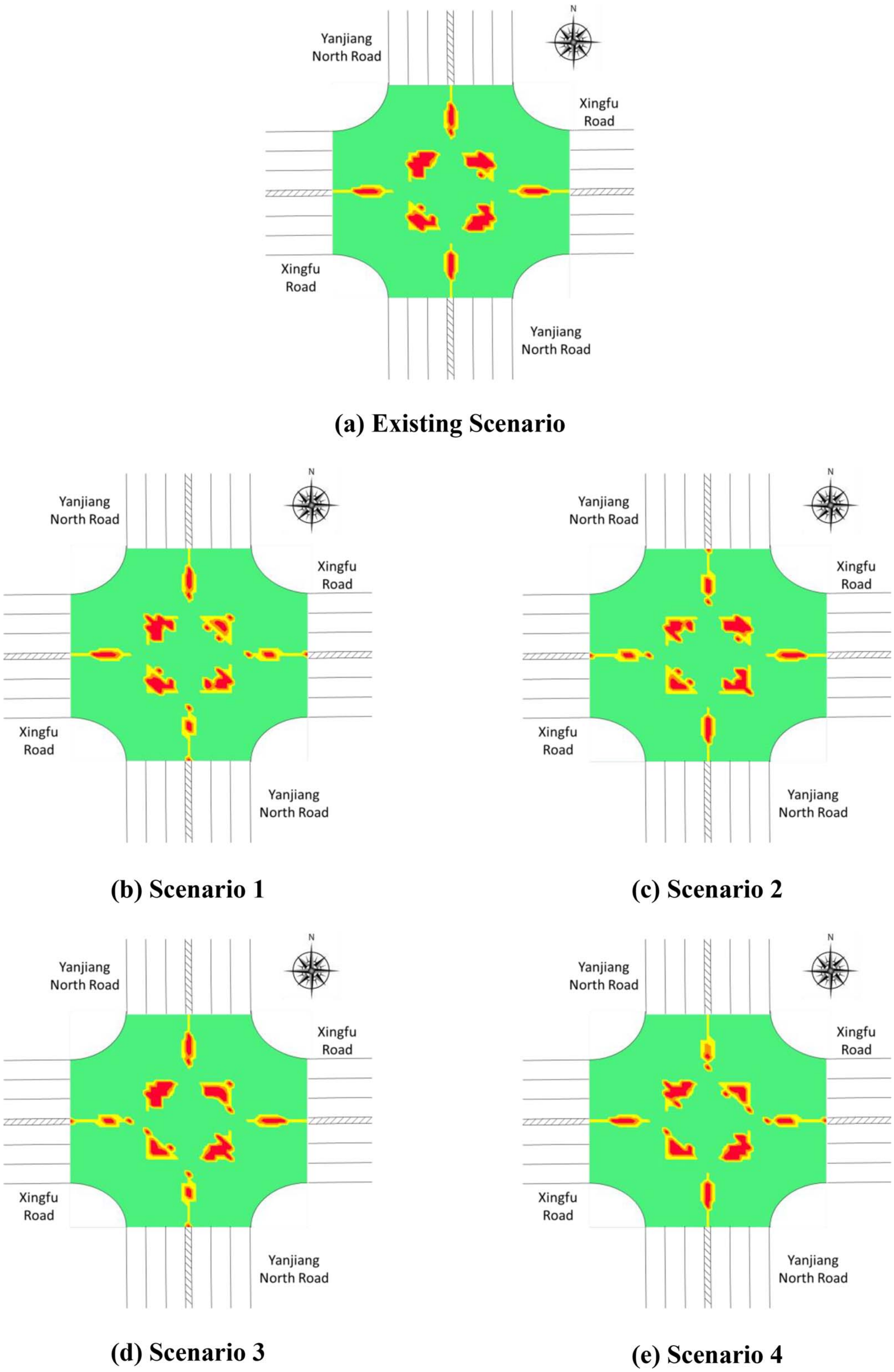

Fig. 7. Safety heatmaps of different flow control scenarios.

changes (Fig. 8(a)). If it is cut through the diagonal (meaning the flow changes of each approach are the same), the figure shows how the overall safety index changes as the approach flow of the entire intersection increases simultaneously (Fig. 8(b)).

It is obvious as shown in Fig. 8(b) that as the flow of each approach increases from 0.02 to 0.1pcu/s, the overall safety index increases sharply. For an intersection formed by two crossing roads, if the flow volume in each direction is less than 180pcu/h, control measures should be taken to guarantee the safety condition of the intersection.

6.3. Turning prohibition

Turning prohibition is the extreme case of flow control measure. Vehicles from two opposite left-turning direction are banned. In reality

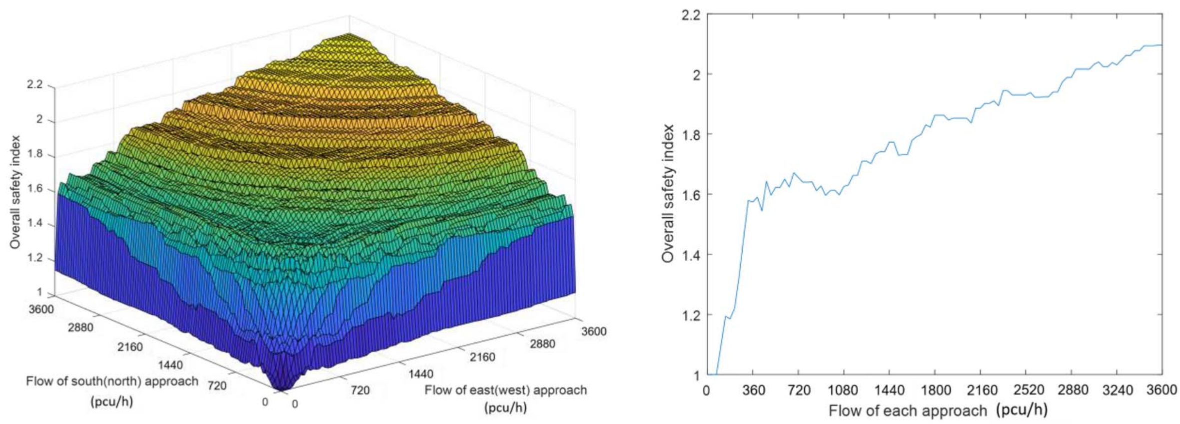

(a) Flow-overall safety index relationship 3D (b) Flow-overall safety index relationship 2D

Fig. 8. Flow-overall safety index relationship.

Table 9
Parameters and safety assessment results of turning prohibition measures.

Turning prohibition scenario (veh/s)												
No.	East approach			West approach			South approach			North approach		
	Left	Straight	Right	Left	Straight	Right	Left	Straight	Right	Left	Straight	Right
0	0.477	0.477	0.477	0.498	0.498	0.498	0.263	0.263	0.263	0.289	0.289	0.289
1	0	0.477	0.477	0	0.498	0.498	0.263	0.263	0.263	0.289	0.289	0.289
2	0.477	0.477	0.477	0.228	0.249	0.218	0	0.263	0.263	0	0.289	0.289

Safety assessment results				
Scenario No.		0 (Existing scenario)	Scenario 1	Scenario 2
Level I	Area(m^2)	1513	1617	1617
	Relative value	1	1	1
Level II	Area(m^2)	95	33	27
	Relative value	0.0628	0.0204	0.0167
Level III	Area(m^2)	7	6	6
	Relative value	0.0046	0.0037	0.0037
Level IV	Area(m^2)	66	25	31
	Relative value	0.0436	0.0155	0.0192
Entire intersection	Total area(m^2)	1681	1681	1681
	Overall index	1.7198	1.2622	1.2845
	Number of conflict areas	8	4	4

management, straight-forward moving vehicles should not be banned because they are the major flow; and it is unnecessary to ban the right-turn flow since it has little influence on intersection congestion and safety. Therefore, left-turn flow is usually banned. Based on this situation, left-turn prohibition scenarios of east-west approach and south-north approach are provided for scenarios 1 and 2. The flow and safety assessment result of each scenario is shown as Table 9 and Fig. 9.

According to the results above, the safety improvement effect resulting from the left-turn prohibition measures is significant. The relative area of the seriously dangerous level is reduced by more than half. In particular for the direction with larger flow, the left-turn prohibition measure not only decreases the overall index by 26.6%, it also helps reduce the conflict area number. The four conflict areas near approaches caused by turning vehicles are eliminated due to this measure.

6.4. Velocity control

Although the design velocity cannot directly reflect the velocity during the actual intersection operation, it will limit the maximum velocity of passing vehicles after the velocity control measure has been conducted. The original design velocity of this intersection and velocity control scenarios with their safety assessment results are shown in Table 10 and Fig. 10. Scenario 1 and 2 separately restrict the velocity of the east-west approach and south-north approach.

The safety improvement of velocity control measure is not ideal, as shown in the results above. Particularly in levels III and IV, the relative areas do not clearly decrease, and may perhaps increase. The most effective scenario, scenario 1, only reduces the overall index by 1.3%.

Regarding the conflict area, the safety measures comparison results are as follows. There are many conflicts under the existing scenario of the intersection; turning prohibition measures sharply decrease the vehicle conflict area within the scope of the intersection. The four conflict areas close to each approach disappear due to prohibition of left-turning vehicles from the west-east direction, resulting in a great reduction in the southwest and northeast conflict areas; other flow control measures reduce the conflicts caused by vehicles traveling in the west and east directions; the result of velocity control is similar to that of the existing scenario. Regarding the safety index, turning prohibition measures exhibit the highest safety level. Although flow and

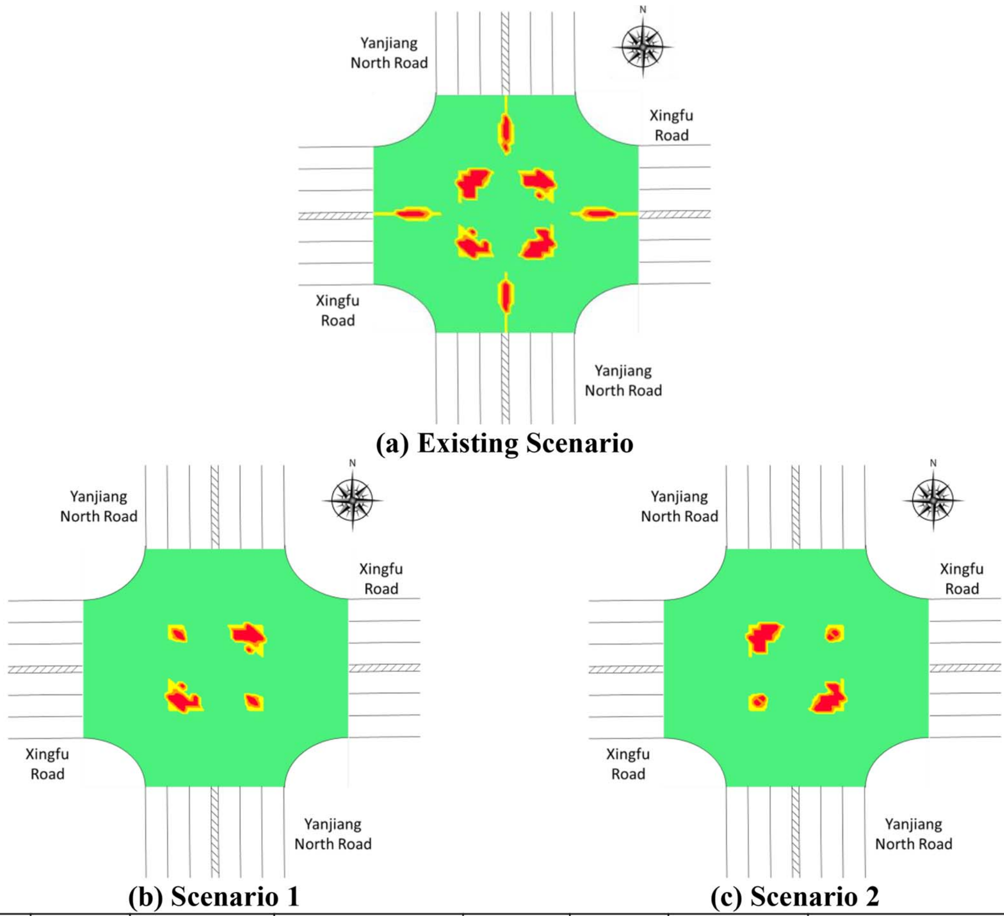

Legend	Color	Safety level	Description	Legend	Color	Safety level	Description
	Green	I	Safe		Orange	III	Dangerous
	Yellow	II	Marginally safe		Red	IV	Seriously dangerous

Fig. 9. Safety heatmaps of different turning prohibition scenarios.

Table 10
Parameter values and safety assessment results of velocity control measures.

Velocity control scenario (km/h)												
No.	East approach			West approach			South approach			North approach		
	Left	Straight	Right	Left	Straight	Right	Left	Straight	Right	Left	Straight	Right
0	35	40	30	35	40	30	35	40	30	35	40	30
1	18	20	15	18	20	15	35	40	30	35	40	30
2	35	40	30	35	40	30	18	20	15	18	20	15

Safety assessment results				
Scenario No.		0 (Existing scenario)	Scenario 1	Scenario 2
Level I	Area(m^2)	1513	1513	1514
	Relative value	1	1	1
Level II	Area(m^2)	95	98	94
	Relative value	0.0628	0.0648	0.0621
Level III	Area(m^2)	7	12	8
	Relative value	0.0046	0.0079	0.053
Level IV	Area(m^2)	66	58	65
	Relative value	0.0436	0.0383	0.0429
Entire intersection	Total area(m^2)	1681	1681	1681
	Overall index	1.7198	1.6980	1.7147
	Number of conflict areas	8	8	8

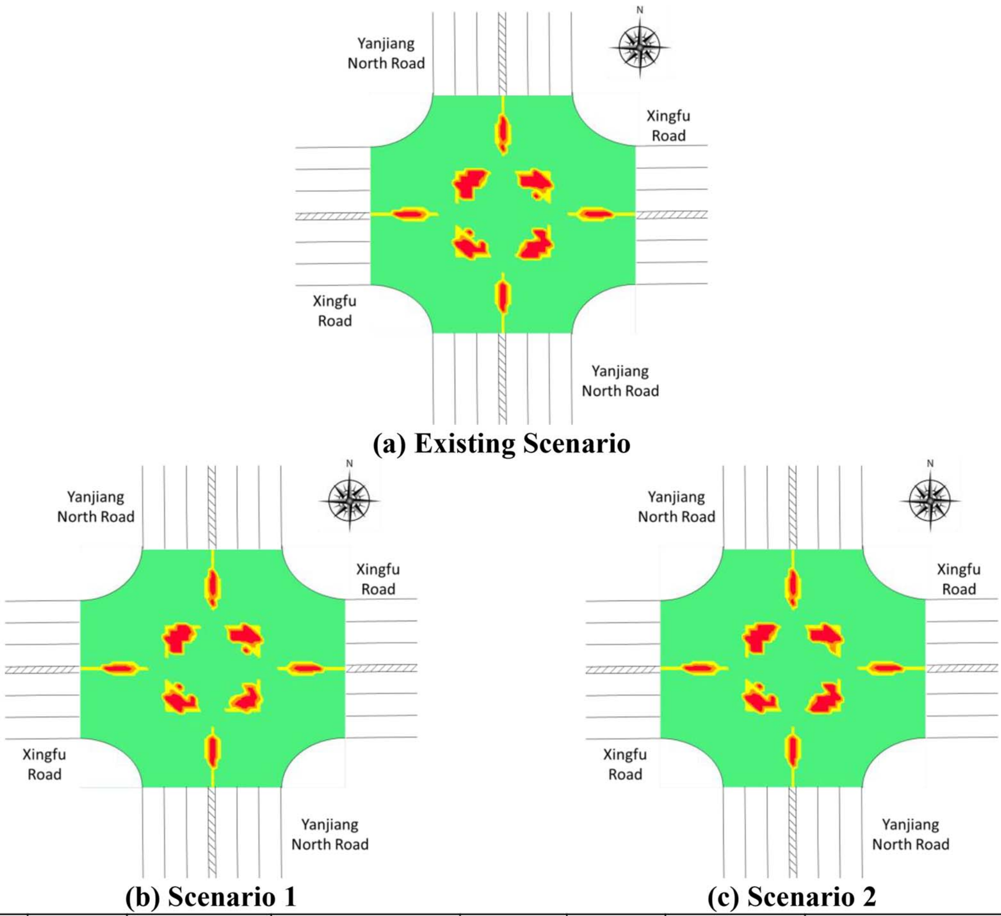

Legend	Color	Safety level	Description	Legend	Color	Safety level	Description
	Green	I	Safe		Orange	III	Dangerous
	Yellow	II	Marginally safe		Red	IV	Seriously dangerous

Fig. 10. Safety heatmaps of different velocity control scenarios.

velocity control are similar in overall safety index, the relative value of flow control is much smaller than velocity control. According to the analysis above, left-turn prohibition is the best alternative among the three measures. Meanwhile, the assessment results indicate that for this intersection, four conflict areas disappeared and the safety level index greatly decreased when only two left-turn flows are prohibited instead of four.

In conclusion, each of the three measures results in some improvement to the safety condition of the intersection. The proposed method can comprehensively assess the effects of alternatives on safety, including the number and distribution of conflict areas, the safety level of each cell and the safety level of the entire intersection. The number of conflict areas is also an influencing factor in the safe operation of the intersection, in addition to the overall safety index. The fewer conflict areas, the easier for drivers to focus on them, improving driving safety. The proposed method performs very well in intersection safety assessment especially for alternative design and improvement measures. In addition, the influence of traffic flow on safety has been confirmed and the suggested flow limitation is proposed.

7. Conclusions

This paper proposes a more effective method of safety assessment for uncontrolled intersections, which can assess not only the safety of an entire intersection but also of the inner spaces of the intersection. The method was based on the analysis of vehicle trajectories within intersections. The cluster assessment method is used to consider both the influence from conflict probability and from conflict severity. The probability included approaching probability and lateral migration probability, which describe the main movement in a lane. Severity uses kinetic energy loss during a crash, which estimates the real loss of conflict.

The case study demonstrates that this safety assessment method is feasible and the visual output of the safety assessment makes it more convenient to achieve the distribution and comparison results, specifically in the following four evaluation areas:

i) **Safety assessment of designed intersections.** This is the most important contribution of this work. The proposed method, which does not require historic crash data, is useful for identifying hidden dangers of the scheme during the design stage, and providing reference for scheme improvement before construction, resulting in crash prevention and cost savings. Previous studies, as far as is known cannot achieve the safety assessment of designed intersection without historic crash data or operation video data. Therefore, the proposed method offers a breakthrough in solving this particular problem.

ii) **Dangerous position management within an intersection.** The distribution of dangerous sites within intersections is invaluable in determining why crashes occur and in formulating countermeasures to improve intersection safety. Most of previous research was only able to assess the safety condition of an intersection as a whole, or one step further, using accident data or predicted conflict point to identify the most probable location where a crash may occur within the intersection. However, the output of the proposed method in this paper assesses the safety level of each area within the intersection and shows the distribution of dangerous positions, making dangerous position management much easier to conduct and its results more specific.

iii) **Safety evaluation of build-up intersections.** The proposed assessment method, which is a proactive approach, requires only the geometry data of intersections and designed or observed traffic volume, velocity and several other parameters related to vehicles, instead of using crash history data, the collection of which is time consuming. The method could also be used to identify hotspot intersections for vehicle conflicts. Compared with previous studies on build-up intersections, the proposed method avoids collecting historic crash data or operation video data, reduces the workload of data collection, and focuses on the safety impact of the build-up intersections facilities or design instead of the crashes themselves.

iv) **Safety level comparison among different intersections or various designs for the same intersection.** Indicators obtained from the proposed method, such as area of each safety level and their relative values, overall safety index and the number of conflict areas within intersections, provide multiple performance metrics to compare intersections or alternatives of a certain intersection from the perspective of traffic safety. The safety evaluation indicators are relatively simple, while the proposed method provides more possibilities of safety level assessment and comparison.

This paper takes a four-leg intersection that has three lanes as an example to demonstrate the methodology. Other types of intersections would use the same application of the proposed approach. Further research will focus on safety assessments of signal-controlled intersections and inter-modes—for example, conflict between vehicles and pedestrians, and vehicles and bicycles. Moreover, instead of using the conflict probability, the behaviors of drivers and pedestrians can be taken into consideration to simulate the operation of the intersection, and build a new kind of safety assessment method.

Conflicts of interest

None.

Acknowledgements

The authors would like to acknowledge the Natural Science Foundation of China (NSFC) (grant No. 51308227) and the Fundamental Research Funds for the Central Universities (201522087) for financial support, the Safe Transportation Research and Education Center at the University of California, Berkeley for providing logistics and administrative support to the scholar exchange program to facilitate this research, and the China Scholarship Council for support of the scholar exchange program. Yunyun Ma, Yifei Shi and Yuchao Cao, undergraduate students at the South China University of Technology, volunteered on the team to assist with data collection and drawing sketches.

References

Alhajyaseen, W., 2015. The integration of conflict probability and severity for the safety assessment of intersections. Arab. J. Sci. Eng. 40 (2), 421–430.
Allen, B.L., Shin, B.T., Cooper, P.J., 1978. Analysis of traffic conflicts and collisions. Transp. Res. Rec. 667, 67–74.
Ceder, Avishai, Eldar, Kobi, 2002. Optimal distance between two branches of uncontrolled split intersection. Transp. Res. Part. A: Policy Pract. 36 (8), 699–724.
Brown, G., Chau, A., Ho, H., et al., 1986. Evaluation of Urban Intersection Improvements Using Traffic Conflicts. Transportation Association of Canada, Ottawa, pp. 68.
Chen, X., Yin, J., 2013. Overview of safety assessment of intersections. Guide Sci. Technol. Mag. 24, 233.
Cheng, W., 2004. Research on the Theory Model and Method of Traffic Accidents and Traffic Conflict Technique in Urban Streets. Jilin University, Changchun.
Cornelissen, M., Salmon, P.M., Stanton, N.A., et al., 2013. Assessing the' system' in safe systems-based road designs: using cognitive work analysis to evaluate intersection designs. Accid. Anal. Prev. 74 (2015), 324–338.
Laureshyn, A., Svensson, A., Hydén, C., 2010. Evaluation of traffic safety, based on micro-level behavioural data: theoretical framework and first implementation. Accid. Anal. Prev. 42 (6), 1637–1646.
Ferreira, S., Couto, A., 2015. A probabilistic approach towards a crash risk assessment of urban segments. Transp. Res. Part C: Emerg. Technol. 50 (50), 97–105.
He, M., Guo, X., Chen, Y., et al., 2010. Application of improved gray clustering method in urban safety assessment. Traff. Inf. Saf. 28 (1), 104–107.
Hu, M., 2009. An empirical study for vehicle arrival statistical distribution at an intersection. Road Traff. Saf. 9 (2), 10–15.
Kaysi, Isam A., Abbany, Ali S., 2007. Modeling aggressive driver behavior at unsignalized intersections. Accid. Anal. Prev. 39 (4), 671–678.
Lin, G., 2010. Analysis on vehicle driver's driving characteristics in lane. J. Highw. Transp. Res. Dev. 27 (10), 101–106.
Lin, Y., Niu, J., Xu, Y., 2011. Study on characteristics of vehicle path in curves on two-lane highways. J. Highw. Transp. Res. Dev. 28 (3), 113–117.
Lorion, A.C., Persaud, B., 2015. Investigation of surrogate measures for safety assessment of urban two-way stop controlled intersections. Can. J. Civil Eng. 42 (12), 987–992.
Lu, G., Liu, M., Wang, Y., et al., 2012. Quantifying the severity of traffic conflict by assuming moving elements as rectangles at intersection. Proc. Soc. Behav. Sci. 43, 255–264.
Lu, J., Pan, F.Q., Xiang, Q.J., 2008. Level-of-safety service for safety performance evaluation of highway intersections. Transp. Res. Rec. 2075, 24–33.
Ma, M., Yan, X., Wu, C., et al., 2010. The effects of principal influential factors on traffic accident frequency at controlled intersections. J. Jilin Univ. (Eng. Technol. Ed.) 40 (2), 417–422.
Minderhoud, M.M., Bovy, P.H.L., 2001. Extended time-to-collision measures for road traffic safety assessment. Accid. Anal. Prev. 33, 89–97.
Niu, H., 2005. Study on safety evaluation of urban road traffic based on gray theory. China Saf. Sci. J. 15 (9), 92–95.
Pei, Y., 2007. Road Traffic Safety. China Communications Press, Beijing.
Qu, L., 2011. Study on Safety Evaluation of Urban Signalized Intersections. Beijing University of Post & Elecommunication: Beijing.
Nagalla, Rakshita, Pothuganti, Prasanna, Pawar, Digvijay S., 2017. Analyzing Gap acceptance behavior at unsignalized intersections using support vector machines, decision tree and random forests. Proc. Comput. Sci. 109, 474–481.
SafeTREC, 2016. Transportation Injury Mapping System. Available from:. http://tims.berkeley.edu/.
Maurya, Akhilesh Kumar, Amin, Harsh J., Kumar, Arvind, 2016. Estimation of critical gap for through movement at four leg uncontrolled intersection. Transp. Res. Proc. 17, 203–212.
Machiani, Sahar Ghanipoor, Abbas, Montasir, 2016. Safety surrogate histograms (SSH): A novel real-time safety assessment of dilemma zone related conflicts at signalized intersections. Accid. Anal. Prev. 96, 361–370.
Sun, J., Zhao, L., 2011. An improved traffic safety simulation method for mixed-traffic intersection. China Saf. Sci. J. 21 (6), 33–37.
Sayed, Tarek, Brown, Gerald, Navin, Francis, 1994. Simulation of traffic conflicts at unsignalized intersections with TSC-Sim. Accid. Anal. Prev. 26 (5), 593–607.
Wang, F., 2013. The design of intersection diversion route. Transp. Sci. Technol. 262, 108–110.
Wang, Y., Huang, X., 2014. Based on the safety service level of urban road singal intersection safety evaluation studies. Highw. Eng. 39 (4), 130–135.
Wang, Y., Yang, S., Pan, B., 2016. Research of vehicle running track in highway straight section. J. Highw. Transp. Res. Dev. 33 (2), 111–119.
Zhang, J., Wang, Y., Wang, J., et al., 2012. Influence law research on collision variables on vehicle collision acute degree. J. Beihua Univ. (Nat. Sci.) 13 (2), 216–220.
Zhang, K., 2012. Study on Safety Assessment of Urban Road and Saftry Measures. Nanjing Forestry University, Nanjing.
Zhang, X., Yang, X., Zhao, J., 2015. A safety evaluation model for unsignalized T-intersections based on conflict probability. Traff. Inf. Saf. 33 (4), 54–68.
Zhou, H., Huang, F., 2013. Development of traffic safety evaluation method based on simulated conflicts at signalized intersections. Proc. Soc. Behav. Sci. 96, 881–885.
Zhou, J., Xu, P., Chai, G., 2008. Intersection safety fuzzy synthetic evaluation based on traffic conflict. Traff. Comput. 26 (2), 123–126.